

## On the Ethanol Electrooxidation Reaction on Catalytic Surfaces of Pt in 0.1 M NaOH

Boguslaw Pierozynski\*

Department of Chemistry, Faculty of Environmental Protection and Agriculture University of Warmia and Mazury in Olsztyn, Plac Lodzki 4, 10-957 Olsztyn, Poland

\*E-mail: [bogpierzynski@yahoo.ca](mailto:bogpierzynski@yahoo.ca)

Received: 21 February 2012 / Accepted: 6 April 2012 / Published: 1 May 2012

---

The present study reports cyclic voltammetric and a.c. impedance spectroscopy investigations of electrooxidation reaction of ethanol on Pt catalytic surfaces, performed in 0.1 M NaOH supporting electrolyte. The kinetics of C<sub>2</sub>H<sub>5</sub>OH oxidation were specifically examined on polycrystalline Pt, Pt(111) and (100) single-crystal surfaces, with special consideration of underpotential deposition (UPD) of H at Pt. In order to study temperature dependence of ethanol oxidation reaction, electrochemical examinations were performed for polycrystalline Pt electrode over the temperature range: 23-60 °C.

---

**Keywords:** Ethanol electrooxidation, UPD of H, Pt single-crystal catalysts, temperature dependence, impedance spectroscopy.

### 1. INTRODUCTION

Electrochemical oxidation of alcohols has a direct application in the so-called DAFC (*Direct Alcohol Fuel Cell*) devices. The most widely studied alcohols for low-temperature PEMFCs (*Proton Exchange Membrane Fuel Cells*) are methanol and ethanol fuels, where the latter one is considered a promising substitute for the former, due to its higher (by *ca.* 30 %) energy-density and non-toxic properties. Ethanol is also a renewable resource, because it can be generated from a variety of available agricultural products and biomass substrates [1-8].

The process of ethanol oxidation on Pt-based (and other) catalytic surfaces is a complex anodic process, which (following C<sub>2</sub>H<sub>5</sub>OH electrosorption step) involves dissociation of ethanol molecules to produce surface-adsorbed CO<sub>ads</sub> species or further oxidation to form acetaldehyde, and acetic acid [2, 9, 10]. A vast group of catalyst materials, including: bulk polycrystalline [3] and various single-crystal

planes of Pt [3, 10-12], PtRu [2, 13], PtRh [2, 9], PtSn [1, 2, 6, 7, 12, 14] and PtPd [8] alloys/co-deposits (typically produced on large surface area C substrates) have extensively been examined (both in acidic and in alkaline media) towards their electrochemical behaviour in ethanol electrooxidation reaction.

Current study represents comprehensive electrochemical investigations of the process of ethanol oxidation on the selected Pt catalytic materials, namely: polycrystalline Pt, Pt(111) and (100) single-crystals in 0.1 M NaOH supporting electrolyte. Kinetic examinations of the oxidation process have been addressed in parallel with the process of underpotential deposition (UPD) of H on Pt, as well as in function of increasing reaction temperature for polycrystalline Pt.

## 2. EXPERIMENTAL

### 2.1. Solutions, electrochemical cell, reference and counter electrodes

High-purity solutions were prepared from water derived from an 18.2 M $\Omega$  Direct- Q3 UV ultra-pure water purification system from Millipore. Aqueous, 0.1 M NaOH solution was prepared from AESAR, 99.996 % NaOH pellets. Ethanol (Stanlab, pure, p.a., Poland) was used to prepare alkaline solutions, at concentrations of 0.25 and 1.0 M C<sub>2</sub>H<sub>5</sub>OH. Before conducting experiments, all solutions were de-aerated with high-purity argon (Ar 6.0 grade, Linde), the flow of which was also maintained above the solutions during the cyclic voltammetry and impedance spectroscopy measurements.

An electrochemical cell, made all of Pyrex glass, was used during the course of this work. The cell comprised three electrodes: a Pt working electrode (WE), equipped with flexible adjustment (in a central part), a reversible Pd hydrogen electrode (RHE) as reference and a Pt counter electrode (CE), both in separate compartments. Prior to each series of experiments, the electrochemical cell was taken apart and soaked in hot sulphuric acid for at least 3 hours. After having been cooled to about 40 °C, the cell was thoroughly rinsed with Millipore ultra-pure water. An identical procedure was applied for cleaning all the glassware used to prepare supporting electrolyte.

The palladium hydrogen electrode, acting as a reversible hydrogen electrode (RHE) was used throughout this work. Hence, all the potentials are given on the RHE scale. The palladium RHE was made of a coiled Pd wire (0.5 mm diameter, 99.9 % purity, Aldrich) and sealed in soft glass. Before its use, this electrode was cleaned in hot sulphuric acid, followed by cathodic charging with hydrogen in 0.5 M H<sub>2</sub>SO<sub>4</sub> (at current,  $I_c = 10$  mA), until H<sub>2</sub> bubbles in the electrolyte were clearly observed. A counter electrode was made of a coiled Pt wire (1.0 mm diameter, 99.9998 % purity, Johnson Matthey, Inc.). Prior to its use, the counter electrode was cleaned in hot sulphuric acid.

### 2.2. Equipment and Pt catalyst materials

Cyclic voltammograms were recorded at 23 °C and over the temperature range: 23 through 60 °C (for the temperature-dependent experiments with polycrystalline Pt), at a sweep-rate of 50 mV s<sup>-1</sup>

by means of the Solartron 12,608 W Full Electrochemical System, consisting of 1260 frequency response analyzer (FRA) and 1287 electrochemical interface (EI). For a.c. impedance measurements (carried-out at 23 °C), the 1260 FRA generator provided an output signal of known amplitude (5 mV) and the frequency range was typically swept between  $1.0 \times 10^5$  and  $0.5 \times 10^{-1}$  Hz. The instruments were controlled by *ZPlot 2.9* or *Corrware 2.9* software for Windows (Scribner Associates, Inc.). Presented here impedance results were obtained through selection and analysis of representative series of experimental data. Typically, three impedance measurements were conducted at each potential value. Reproducibility of such-obtained results was usually below 10 % from one measurement to another. The impedance data analysis was performed with *ZView 2.9* software package, where the spectra were fitted by means of a complex, non-linear, least-squares imittance fitting program, *LEVM 6*, written by Macdonald [15]. Four equivalent circuits for identified charge-transfer surface processes, including constant-phase elements (CPEs) to account for distributed capacitance were employed to analyze the obtained impedance results, as later shown in Figs. 5a through 5d below.

Polycrystalline Pt and Pt single-crystals of the (111) and (100) orientations were made from 1 mm diameter 99.9985 % Pt wire (AESAR/Puratronic). Single-crystal electrodes were prepared by employing the techniques and procedures for preparation of Pt single-crystals, developed by Clavilier et al. [16-19], where the crystals' orientations were determined by means of the back von Laue X-ray diffraction method [20, 21].

### 3. RESULTS AND DISCUSSION

#### 3.1. Electrooxidation of ethanol - cyclic voltammetry

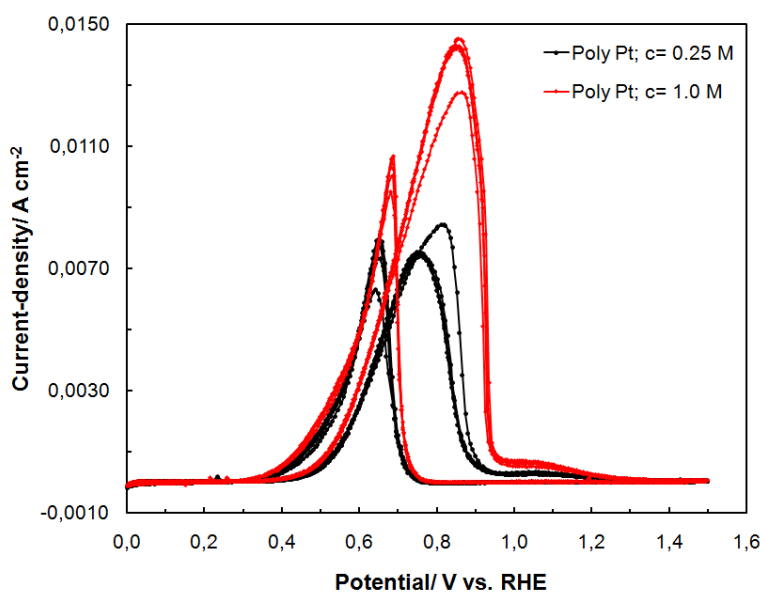


**Figure 1.** Cyclic voltammograms for ethanol electrooxidation on polycrystalline Pt electrode, carried-out in 0.1 M NaOH, at a sweep-rate of  $50 \text{ mV s}^{-1}$  and in the presence of 0.25, and 1.0 M  $\text{C}_2\text{H}_5\text{OH}$  (five consecutive cycles were recorded for each CV run).

The cyclic voltammetric behaviour of the process of electrooxidation of ethanol on polycrystalline Pt electrode surface in 0.1 M NaOH is shown in Fig. 1. Thus, a single oxidation peak, centred at *ca.* 0.80 V vs. RHE appears upon an anodic sweep; however, when the CV sweep is reversed towards the H<sub>2</sub> reversible potential, another oxidation peak (centred at *ca.* 0.65 V) emerges in the voltammetric profile (Fig. 1). While the latter peak is typically attributed to the process of oxidation of surface-adsorbed CO<sub>ads</sub> species, the former one is usually assigned to the formation of acetaldehyde [3, 10, 11]. Moreover, electrooxidation of ethanol on the Pt surface takes part in parallel with the process of UPD of H, which arises in alkaline media at Pt over the potential range *ca.* 50-400 mV vs. RHE. However, it can be seen in the respective CV profile of Fig. 1 that a 4-fold increase of ethanol concentration (from 0.25 to 1.0 M C<sub>2</sub>H<sub>5</sub>OH) resulted in significantly intensified voltammetric current-densities.

Although the recorded behaviour at Pt(100) plane was similar to that observed for polycrystalline Pt, considerably enhanced catalytic activity towards ethanol oxidation was observed at Pt(111) single-crystal surface (see Fig. 2 below).

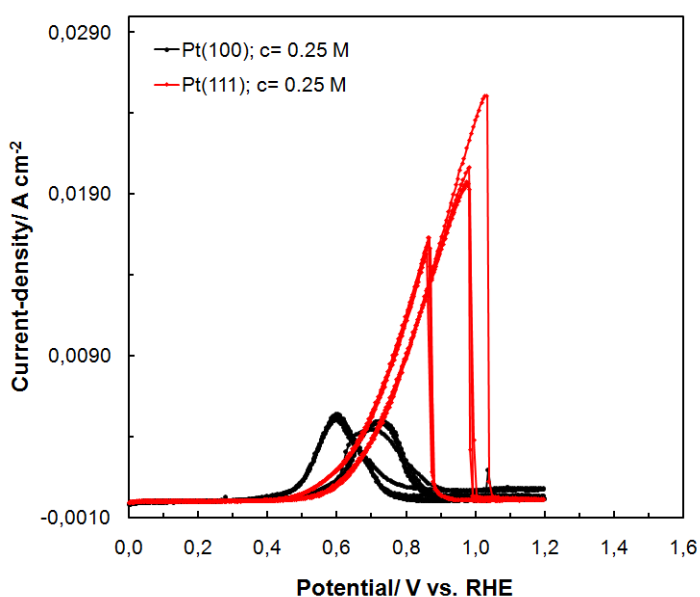


**Figure 2.** Cyclic voltammograms for ethanol electrooxidation on Pt(111) and (100) single-crystal surfaces, carried-out in 0.1 M NaOH, at a sweep-rate of 50 mV s<sup>-1</sup> and in the presence of 0.25 M C<sub>2</sub>H<sub>5</sub>OH (five consecutive cycles were recorded for each CV run).

Here, under similar experimental conditions (at 0.25 M C<sub>2</sub>H<sub>5</sub>OH), the recorded maximum of oxidation current-density at *ca.* 1.0 V was about 3 times as high as the corresponding value for the polycrystalline Pt electrode (see Fig. 1 again). It is strongly believed that the above-observed behaviour is related to the extent of OH adsorption on the respective Pt single-crystal planes. Please note that in alkaline media, the Pt(111) surface is the only basal plane, where the UPD H region is widely separated from that for adsorption of OH<sup>-</sup> anions by a double-layer charging zone. Conversely,

on the Pt(100) plane, desorption of H is immediately followed by the adsorption of oxygen-like species and these two processes evidently overlap [22-24].

3.2. Electrooxidation of ethanol - a.c. impedance spectroscopy

The a.c. impedance spectroscopy behaviour of the process of electrooxidation of ethanol (in the presence of UPD of H) on the three selected Pt catalyst materials in 0.1 M NaOH is presented in Tables 1 and 2, and in Figs. 3 and 4 below.

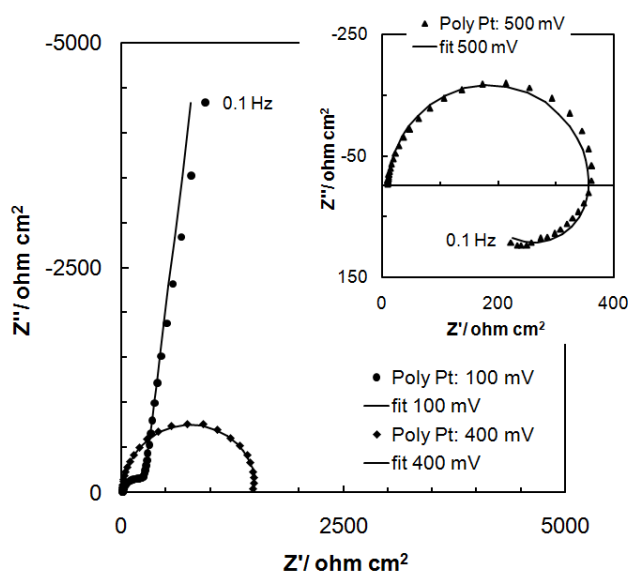


**Figure 3.** Complex-plane impedance plots for polycrystalline Pt in contact with 0.1 M NaOH, in the presence of 0.25 M  $\text{C}_2\text{H}_5\text{OH}$ , recorded at the stated potential values (at 23 °C). The solid line corresponds to representation of the data according to the equivalent circuits shown in Figs. 5b, 5c and 5d.

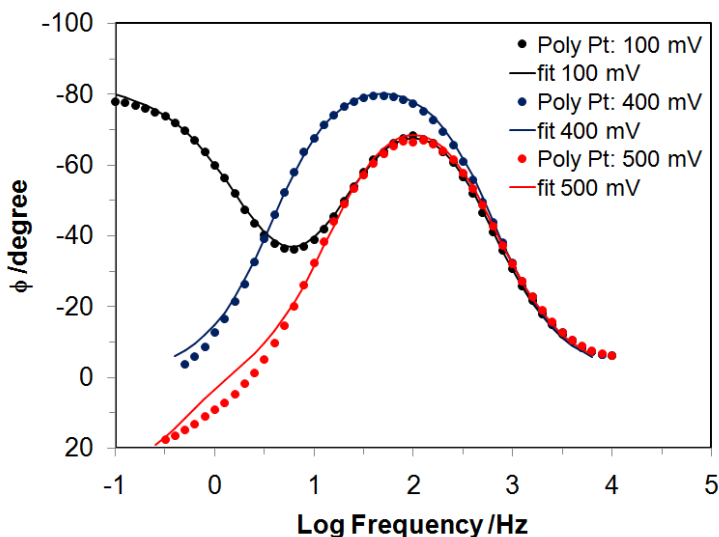


**Figure 4.** Bode phase-angle plots (other details as in Fig. 3 above).

**Table 1.** Resistance and capacitance parameters for electrooxidation of ethanol (at 0.25 and 1.0 M C<sub>2</sub>H<sub>5</sub>OH) and UPD of H on polycrystalline Pt electrode in 0.1 M NaOH (at 23 °C), obtained by finding the equivalent circuits which best fitted the impedance data, as shown in Figs. 5b<sup>b</sup>, 5c<sup>c</sup> and 5d<sup>d</sup>.

E/ mV	R <sub>H</sub> / Ω cm <sup>2</sup>	x10 <sup>6</sup> C <sub>pH</sub> / F cm <sup>-2</sup> s <sup>φ1-1</sup>	x10 <sup>6</sup> C <sub>dl</sub> / F cm <sup>-2</sup> s <sup>φ2-1</sup>	R <sub>ct</sub> / Ω cm <sup>2</sup>
0.25 M C <sub>2</sub> H <sub>5</sub> OH				
100 <sup>c</sup>	303.6 ± 2.0	315.4 ± 1.2	37.4 ± 0.5	-----
200 <sup>c</sup>	844.3 ± 18.6	192.0 ± 1.7	36.3 ± 0.7	-----
250 <sup>c</sup>	2,585 ± 101	69.1 ± 0.5	33.0 ± 0.3	-----
400 <sup>b</sup>	-----	-----	28.4 ± 0.4	1,520 ± 10
	R <sub>o</sub> / Ω cm <sup>2</sup>	L/ H		
500 <sup>d</sup>	293.3 ± 22.3	521.6 ± 27.3	35.5 ± 1.6	352.5 ± 4.6
1.0 M C <sub>2</sub> H <sub>5</sub> OH				
100 <sup>c</sup>	316.5 ± 2.7	273.7 ± 1.5	35.2 ± 0.6	-----
200 <sup>c</sup>	1,196 ± 23	127.3 ± 1.0	35.7 ± 0.6	-----
250 <sup>c</sup>	1,842 ± 20	72.7 ± 1.3	31.8 ± 1.1	-----
400 <sup>b</sup>	-----	-----	26.2 ± 0.4	1,272 ± 11
	R <sub>o</sub> / Ω cm <sup>2</sup>	L/ H		
500 <sup>d</sup>	310.4 ± 23.3	285.4 ± 15.2	33.2 ± 1.4	300.3 ± 3.6

**Table 2.** Resistance and capacitance parameters for electrooxidation of ethanol (at 0.25 M C<sub>2</sub>H<sub>5</sub>OH) and UPD of H on Pt(111) and (100) electrode surfaces in 0.1 M NaOH (at 23 °C), obtained by finding the equivalent circuits which best fitted the impedance data, as shown in Figs. 5a<sup>a</sup> through 5d<sup>d</sup>.

E/ mV	R <sub>H</sub> / Ω cm <sup>2</sup>	x10 <sup>6</sup> C <sub>pH</sub> / F cm <sup>-2</sup> s <sup>φ1-1</sup>	x10 <sup>6</sup> C <sub>dl</sub> / F cm <sup>-2</sup> s <sup>φ2-1</sup>	R <sub>ct</sub> / Ω cm <sup>2</sup>
Pt (111)				
100 <sup>c</sup>	110.6 ± 1.1	574.9 ± 4.2	36.8 ± 1.3	-----
200 <sup>c</sup>	112.9 ± 0.9	537.6 ± 3.3	41.6 ± 1.2	-----
300 <sup>c</sup>	235.6 ± 6.1	141.6 ± 2.7	39.7 ± 1.7	-----
400 <sup>b</sup>	-----	-----	36.8 ± 0.3	11,586 ± 394
450 <sup>b</sup>	-----	-----	30.6 ± 0.4	3,531 ± 38
500 <sup>b</sup>	-----	-----	33.2 ± 0.5	1,251 ± 12
550 <sup>b</sup>	-----	-----	44.3 ± 1.4	489.3 ± 6.5
600 <sup>b</sup>	-----	-----	52.5 ± 1.4	362.7 ± 5.0
700 <sup>b</sup>	-----	-----	153.1 ± 6.4	34.7 ± 0.3
800 <sup>b</sup>	-----	-----	538.2 ± 19.9	82.3 ± 2.0
Pt (100)				
100 <sup>c</sup>	46.6 ± 1.2	492.2 ± 3.9	51.3 ± 4.2	-----
200 <sup>c</sup>	106.5 ± 1.3	326.6 ± 5.8	50.4 ± 1.7	-----
300 <sup>a</sup>	696.0 ± 20.2	86.9 ± 2.5	47.4 ± 1.1	14,836 ± 890
400 <sup>b</sup>	-----	-----	44.0 ± 0.8	2,453 ± 36
450 <sup>b</sup>	-----	-----	46.9 ± 0.8	1,010 ± 15
	R <sub>o</sub> / Ω cm <sup>2</sup>	L/ H		
500 <sup>d</sup>	479.0 ± 29.0	6,458 ± 278	45.3 ± 1.4	698.8 ± 11.0
550 <sup>d</sup>	258.4 ± 21.4	3,564 ± 140	42.0 ± 2.0	1,008 ± 30
600 <sup>d</sup>	226.3 ± 20.8	1,585 ± 73	40.5 ± 2.7	2,405 ± 228

Hence, over the potential range: 100-250 mV vs. RHE, the impedance behaviour of polycrystalline Pt (at 0.25 M C<sub>2</sub>H<sub>5</sub>OH) is characterized by a single, partial semicircle (present over high frequencies) and a capacitive line, at an inclination to the Z' axis different from 90°, in the Nyquist impedance spectra (see as an example an impedance spectrum obtained at 100 mV in Fig. 3 and a corresponding Bode phase-angle plot in Fig. 4). This semicircle corresponds to the charge-transfer resistance (R<sub>H</sub>) of the process of UPD of H on Pt. Thus, the R<sub>H</sub> parameter reaches its minimum value of 303.6 Ω cm<sup>2</sup> at 100 mV. Then, upon potential augmentation, the charge-transfer resistance dramatically increases, reaching a very large value of 2,585 Ω cm<sup>2</sup> at the potential of 250 mV (see Table 1). Furthermore, the hydrogen adsorption pseudocapacitance (C<sub>pH</sub>) parameter radically declines from the recorded value of 315.4 (at 100 mV) to 69.1 μF cm<sup>-2</sup> s<sup>φ<sub>1</sub>-1</sup> (at 250 mV), which closely reflects the changes of the R<sub>H</sub> parameter. The onset of ethanol oxidation could already be observed at 300 mV vs. RHE. However, a large-diameter semicircle (in reference to electrooxidation of C<sub>2</sub>H<sub>5</sub>OH, also see the respective R<sub>ct</sub> parameter in Table 1) becomes clearly present throughout the intermediate frequency range in the Nyquist impedance spectrum, recorded at 400 mV (see Figs. 3 and 4). At 500 mV, the charge-transfer resistance of 352.5 Ω cm<sup>2</sup> was recorded and the corresponding Nyquist impedance spectrum exhibited an inductive loop over the low frequency end (see inset in Fig. 3 and Fig. 4). This behaviour is similar to that reported by other authors for ethanol electrooxidation on Pt-based composite materials (see e.g. Refs. 6 and 8). The presence of the inductive loop at the potential of 500 mV (also see associated inductive resistance, R<sub>o</sub> and inductance, L parameters in Table 1) is most likely associated with the process of oxidative removal of CO<sub>ads</sub> species from the Pt surface, leading simultaneously to the release of Pt active sites.

In addition, increased alcohol concentration (from 0.25 to 1.0 M C<sub>2</sub>H<sub>5</sub>OH) significantly facilitated the kinetics of the oxidation process, leading (comparatively) to reduction of the minimum value of the R<sub>ct</sub> parameter (at 500 mV) by a factor of *ca.* 1.2 (Table 1). However, higher concentration of ethanol in the electrolyte cannot explain considerable fluctuation of the recorded charge-transfer resistance parameter for the process of UPD of H.

On the other hand, the double-layer capacitance (C<sub>dl</sub>) parameter exhibited some, but rather insignificant fluctuation (from 26.2 to 37.4 μF cm<sup>-2</sup> s<sup>φ<sub>2</sub>-1</sup>), which is fairly close to that commonly used value of 20 μF cm<sup>-2</sup> in literature for smooth and homogeneous surfaces [25, 26]. Furthermore, a deviation from the purely capacitive behaviour (which required the use of the CPE components in the equivalent circuits, see Figs. 5a through 5d) corresponds to distribution (dispersion) of capacitance. This effect is typically assigned to slow ion adsorption-desorption processes (as previously suggested by Pajkossy [27]) or to increasing surface inhomogeneity, being a possible result of prolonged potentiostatic impedance measurements [27-29]. In this work, values of dimensionless parameters φ<sub>1</sub> and φ<sub>2</sub> (for the CPE components) oscillated between 0.92 and 0.99.

Application of Pt(100) single-crystal electrode did not lead to enhancement of the process of ethanol electrooxidation. On the contrary, for the Pt(100) plane, the minimum charge-transfer resistance value of 698.8 Ω cm<sup>2</sup> was recorded at 500 mV (for 0.25 M C<sub>2</sub>H<sub>5</sub>OH), which was *ca.* twice as high (see Table 2) as that recorded under similar experimental conditions for the polycrystalline Pt electrode (also compare the respective voltammograms in Figs. 1 and 2).

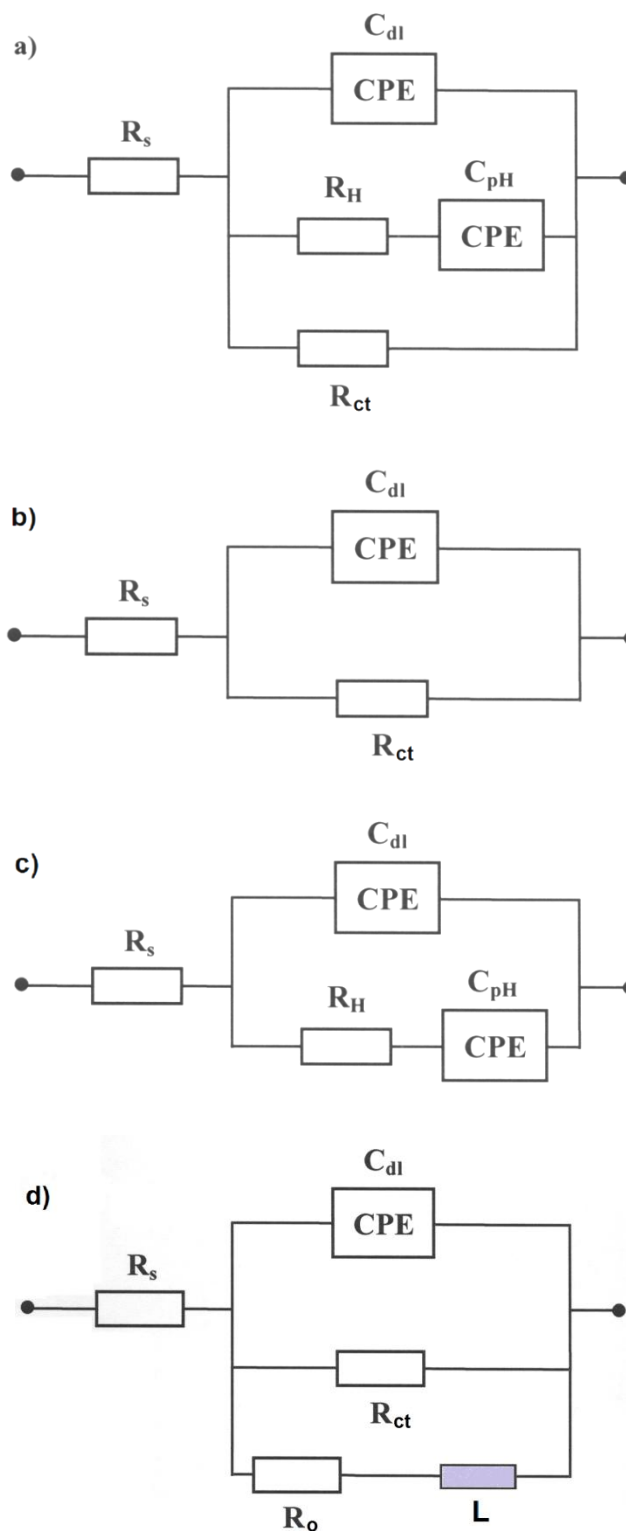


**Figure 5.** Four equivalent circuits, used for fitting the obtained a.c. impedance spectroscopy data in this work, where:  $R_s$  is solution resistance,  $C_{dl}$  is double-layer capacitance,  $R_H$  and  $C_{pH}$  are resistance and pseudocapacitance parameters for the process of UPD of H,  $R_{ct}$  is charge-transfer resistance parameter for electrooxidation of ethanol,  $R_o$  and  $L$  are inductive resistance and inductance parameters, respectively. The circuits include two constant phase elements (CPEs) to account for distributed capacitance.

In addition, dramatic reduction of the inductance (L) parameter, also accompanied by significantly decreased inductive resistance,  $R_o$  (as observed over the potential range: 500-600 mV in Table 2) reflects facilitation of the process of oxidative removal of  $CO_{ads}$  species from the Pt(100) catalyst surface.

Conversely, dramatic enhancement of ethanol electrooxidation reaction was recorded at the Pt(111) plane. Here, minimum of the respective  $R_{ct}$  parameter came to  $34.7 \Omega \text{ cm}^2$  at 700 mV (Table 2), which corresponds to *ca.* 20-fold reduction of the charge-transfer resistance, as compared to the (100) case. Interestingly, no inductive type behaviour in the Nyquist impedance plots was observed for this Pt plane. Please note that these results are in opposition to those recently obtained for electrooxidation of ethanol (in 0.5 M  $H_2SO_4$ ) on these two Pt planes by Pierozynski in Ref. 30. The above is very likely the effect of anion adsorption, where in alkaline media, the Pt(111) surface is the only low-index Pt plane, where the UPD H region is widely separated from that for adsorption of  $OH^-$  anions by a double-layer charging zone (contrast to the behaviour in  $H_2SO_4$ ). In other words, in NaOH, electrosorption (and electrooxidation) of ethanol molecules proceeds on the Pt(111) plane in the relative absence of OH electrosorption.

In addition, the rates for UPD of H on the (111) plane, recorded in Table 2 over the potential range: 100-300 mV, are comparable with those reported by Schouten et al. in Ref. 31 on the kinetics of UPD of H at Pt(111) in 0.05 M NaOH, as well as with the author's own findings, as recently reported in Ref. 32. However, a significant increase of the  $R_H$  to  $235.6 \Omega \text{ cm}^2$  at 300 mV (Table 2) indicates the onset of ethanol electro-sorption(oxidation) reaction. Similar sequence of  $R_H$  parameter values was recorded for the Pt(100) plane in Table 2, where the  $R_H$  increased from 46.6 (at 100 mV) to  $696.0 \Omega \text{ cm}^2$  at 300 mV (compare with the corresponding values of the adsorption pseudocapacitance,  $C_{pH}$  parameter: 492.2 and  $86.9 \mu\text{F cm}^{-2} \text{ s}^{\phi_1-1}$ , respectively). These values of the  $R_H$  parameter are considerably greater than those recorded under similar conditions for the (100) plane in 0.5 M  $H_2SO_4$  [30], which indicates that the kinetics of UPD of H become greatly inhibited in alkaline media.

Again, the recorded in Table 2 double-layer capacitance parameter exhibited fluctuation, between *ca.* 31 and  $52 \mu\text{F cm}^{-2} \text{ s}^{\phi_2-1}$ , whereas those of the dimensionless parameters ( $\phi_1$  and  $\phi_2$  in Table 2) were between 0.93 and 0.98. On the other hand, a dramatic increase of the  $C_{dl}$  parameter, recorded for the (111) plane for potentials beyond 600 mV, implies considerable contribution from another surface adsorption process(es), likely involving reaction intermediates.

Moreover, the process of electrooxidation of ethanol exhibited considerable temperature-dependence. Fig. 6 below presents an Arrhenius plot for ethanol oxidation (at 0.25 M  $C_2H_5OH$ ) on the polycrystalline Pt electrode, recorded for the peak anodic current-density value (also refer to Fig. 1), over the temperature range: 23-60 °C. Thus, augmentation of the reaction temperature led to a significant increase of the recorded voltammetric oxidation current-densities. The Arrhenius plot-derived apparent activation energy ( $E_A$ ) for electrooxidation of ethanol on polycrystalline Pt in 0.1 M NaOH came to  $23.5 \text{ kJ mol}^{-1}$ . This value is in good agreement with those previously recorded for different Pt-based catalyst materials [6, 8, 9], as well as with that recently presented for a bulk polycrystalline Pt material in 0.5 M  $H_2SO_4$  [30].

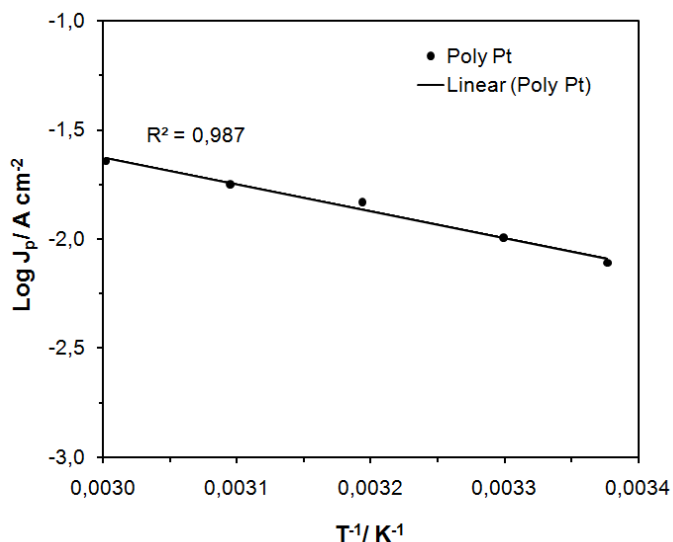


**Figure 6.** Arrhenius plot for ethanol electrooxidation (at 0.25 M  $C_2H_5OH$ ) on polycrystalline Pt electrode in contact with 0.1 M NaOH, recorded for the anodic peak current-density potential value.

#### 4. CONCLUSIONS

The process of electrooxidation of ethanol (carried-out in 0.1 M NaOH supporting electrolyte) proved to be highly specific to geometry of Pt single-crystal catalysts, where Pt(111) plane exhibited significantly enhanced catalytic properties towards ethanol oxidation, as compared to those demonstrated by Pt(100) surface or a polycrystalline Pt electrode material. This is because in alkaline medium (such as 0.1 M NaOH), Pt(111) surface is the only low index Pt plane, where the UPD H region is widely separated from that for adsorption of  $OH^-$  anions by a double-layer charging zone (contrast to the behaviour in  $H_2SO_4$ ). Thus, in NaOH, electrosorption (and electrooxidation) of ethanol molecules proceeds on this Pt plane in the relative absence of electrosorption of OH species. The onset of ethanol oxidation extends over the potential range characteristic to the reversible deposition (UPD) of H on Pt. The presence of ethanol molecules (or reaction intermediates) on the surface of Pt catalyst can significantly affect the rates for UPD of H. Kinetics of ethanol electrooxidation on the Pt catalyst surface are strongly dependent on the reaction temperature, as well as on the concentration of ethanol in sodium hydroxide.

#### ACKNOWLEDGEMENTS

This work has been financed by the strategic program of the National (Polish) Centre for Research and Development (NCBiR): „Advanced Technologies for Energy Generation. Task 4: Elaboration of Integrated Technologies for the Production of Fuels and Energy from Biomass, Agricultural Waste and other Waste Materials”.

## References

1. S. Rousseau, C. Coutanceau, C. Lamy and J.M. Leger, *J. Power Sources*, 158 (2006) 18.
2. S.Q. Song, W.J. Zhou, Z.H. Zhou, L.H. Jiang, G.Q. Sun, Q. Xin, V. Leontidis, S. Kontou and P. Tsiakaras, *Int. J. Hydrogen Energy*, 30 (2005) 995.
3. A.A. Abd-El-Latif, E. Mostafa, S. Huxter, G. Attard and H. Baltruschat, *Electrochim. Acta*, 55 (2010) 7951.
4. S.B. Han, Y.J. Song, J.M. Lee, J.Y. Kim and K.W. Park, *Electrochem. Commun.*, 10 (2008) 1044.
5. M.H. Shao and R.R. Adzic, *Electrochim. Acta*, 50 (2005) 2415.
6. S.S. Gupta, S. Singh and J. Datta, *Mat. Chem. Phys.*, 120 (2010) 682.
7. E.E. Switzer, T.S. Olson, A.K. Datye, P. Atanassov, M.R. Hibbs and C.J. Cornelius, *Electrochim. Acta*, 54 (2009) 989.
8. S.S. Mahapatra, A. Dutta and J. Datta, *Electrochim. Acta*, 55 (2010) 9097.
9. S.S. Gupta and J. Datta, *J. Electroanal. Chem.*, 594 (2006) 65.
10. X.H. Xia, H.D. Liess and T. Iwasita, *J. Electroanal. Chem.*, 437 (1997) 233.
11. J.F. Gomes, B. Busson, A. Tadjeddine and G. Tremiliosi-Filho, *Electrochim. Acta*, 53 (2008) 6899.
12. A.A. El-Shafei and M. Eiswirth, *Surf. Sci.*, 604 (2010) 862.
13. N. Fujiwara, Z. Siroma, S. Yamazaki, T. Ioroi, H. Senoh and K. Yasuda, *J. Power Sources*, 185 (2008) 621.
14. F.C. Simoes, D.M. dos Ajos, F. Vigier, J.M. Leger, F. Hahn, C. Coutanceau, E.R. Gonzalez, G. Tremiliosi-Filho, A.R. de Andrade, P. Olivi and K.B. Kokoh, *J. Power Sources*, 167 (2007) 1.
15. J. R. Macdonald, *Impedance Spectroscopy, Emphasizing Solid Materials and Systems*, John Wiley & Sons, Inc., New York, (1987).
16. J. Clavilier and R. Pineaux, *C.R. Acad. Sci. Paris*, 260 (1965) 891.
17. J. Clavilier, *J. Electroanal. Chem.*, 107 (1980) 211.
18. J. Clavilier, R. Faure, D. Guinet and R. Durand, *J. Electroanal. Chem.*, 107 (1980) 205.
19. J. Clavilier, K. El Achi, M. Petit, A. Rodes and M.A. Zamakhchari, *J. Electroanal. Chem.*, 295 (1990) 333.
20. C.S. Barret and T.B. Massalski, "Structure of Metals: Crystallographic Methods, Principles and Data", McGraw Hill, London, (1966).
21. A. Hamelin in "Modern Aspects of Electrochemistry", B.E. Conway, J.O'M. Bockris and R.E. White (Eds.), Plenum Press, New York, 1 (1985) 16.
22. N.M. Markovic, S.T. Sarraf, H.A. Gasteiger and P.N. Ross, Jr., *J. Chem. Soc., Faraday Trans.*, 92 (1996) 3719.
23. D.F. van der Vliet and M.T.M. Koper, *Surf. Sci.*, 604 (2010) 1912.
24. D.M. Drazic, A.V. Tripkovic, K.D. Popovic and J.D. Lovic, *J. Electroanal. Chem.*, 466 (1999) 155.
25. A. Lasia and A. Rami, *J. Applied Electrochem.*, 22 (1992) 376.
26. L. Chen and A. Lasia, *J. Electrochem. Soc.*, 138 (1991) 3321.
27. T. Pajkossy, *J. Electroanal. Chem.*, 364 (1994) 111.
28. B.E. Conway in *Impedance Spectroscopy. Theory, Experiment, and Applications*, E. Barsoukov and J. Ross Macdonald (Eds.), Wiley-Interscience, John Wiley & Sons, Inc., Hoboken, N.J., 4.5.3.8 (2005) 494.
29. W.G. Pell, A. Zolfaghari and B.E. Conway, *J. Electroanal. Chem.*, 532 (2002) 13.
30. B. Pierozynski, *Int. J. Electrochem. Sci.*, 7 (2012) (in press).
31. K.J. Schouten, M.J. van der Niet and M.T. Koper, *Phys. Chem. Chem. Phys.*, 12 (2010) 15217.
32. B. Pierozynski and I.M. Kowalski, *J. Electroanal. Chem.*, 662 (2011) 432.